Preprints of the 21st IFAC World Congress (Virtual)
Berlin, Germany, July 12-17, 2020

Gray-Box Model Identification and Payload Estimation for Delta Robots ⋆

Fabio Falezza *, **Federico Vesentini** *,
Alessandro Di Flumeri **, **Luca Leopardi** **, **Gianni Fiori** **
Gianfrancesco Mistrorigo **, **Riccardo Muradore** *

* *Dept. of Computer Science, University of Verona, Verona, Italy*
(e-mail: {fabio.falezza,federico.vesentini,riccardo.muradore}@univr.it)
** *SIPRO s.r.l, Verona, Italy*
(e-mail:
{alessandro.diflumeri,luca.leopardi,gianni.fiori,mistrorigo}@sipro.vr.it)

Abstract: Delta Robots belong to a class of parallel robots widely used in industrial production processes, mostly for pick-and-place operations. The most relevant characteristics are the high speed and the extremely favorable ratio between the maximum payload and the weight of the robot itself. A reliable dynamic model is needed to implement torque controllers that reduce unnecessary high accelerations and so mechanical vibrations. Moreover, when the mass of the pickable object is unknown, it is crucial to identify with sufficient precision the dynamic contribution of the payload and to accordingly adapt the dynamic model in order to guarantee high performance.

Keywords: Robot dynamical model, Model Identification, Payload estimation, Delta Robots.

1. INTRODUCTION

Parallel robots are widely used in industrial applications due to their stable functioning, control on the limits of velocities and accelerations, good positional precision and more rigid structure than serial counterparts. In the specific case of Delta robots, they are mechanically robust and can move objects of considerable mass and dimension at high speeds, Staicu and Carp-Ciocardia (2003), Bortoff (2018). Delta robot has a mechanical parallel structure with a closed kinematic chain connecting a fixed platform to the end-effector, as shown in Fig. 1. The end-effector moves in the work-space using three serial kinematic chains with 3 degrees of freedom (DOF). Each serial chain consists of two rigid links connected by a 2-DOF revolute passive joint. Three drives, attached to the fixed base, actuate the first link of each chain. The dynamic models of Delta robots in the literature are currently approximations of the real rigorous model, due to the presence of only three actuated and sensed joints out of nine and a complex kinematic structure with holonomic constraints, whose introduction into the model would increase the mathematical and computational complexity. Kuo and Huang (2017), Kuo (2016) proposed a dynamic model with the first link modeled as a rigid homogeneous bar and the second link as a point mass placed at the end of the first link. This assumption brings to a model relatively easy to handle. On the other hand, it does not take into account a significant part of inertia and potential energy. This paper presents an improvement to the state of art dynamic model of 3-DOF Delta robots using gray-box dynamical parameter identification, friction modelling, and payload identification. The improved mathematical model is validated by using an industrial Delta robot. The paper is organized as follows. Section 2 recalls the robot geometric representation, forward and inverse kinematics model, velocities and acceleration computation. Section 3 introduces the robot dynamic model. Section 4 explains our contributions to enhance the accuracy of the dynamic model in free motion. In particular, gray-box dynamic parameter identification and friction modeling are presented. Section 5 shows a method to estimate the payload in real-time. In Section 6 the final dynamic model and the real dynamic model are compared. The mean error and the standard deviation between the torque profiles on different trajectories will prove the effectiveness of our model.

⋆ This work was partly supported by the project MIUR "Department of Excellence" 2018-2022.

2. KINEMATIC MODEL

The Delta robot is represented (Fig. 1) as a rigid fixed platform $F_1F_2F_3$, connected via three sets of kinematic chains to a rigid moving platform $E_1E_2E_3$. Each chain consists of two rigid links F_iJ_i and J_iE_i, with $i \in \{1, 2, 3\}$, connected by a 2-DOF revolute joint in J_i. Motor drives are fixed on points F_i of the base frame and change the angle θ_i. The origin O of the global reference frame system XYZ is located at the circumcenter of the base frame. The point E_0 is the end-effector position and it is placed in the circumcenter of the moving platform. Commonly the link J_iE_i is modeled as a two-bar parallel mechanism to increase mechanical robustness. In the present work, it will be considered, without loss of generality, as two rigid links with two 2-DOF spherical joints on points J_i and E_i.

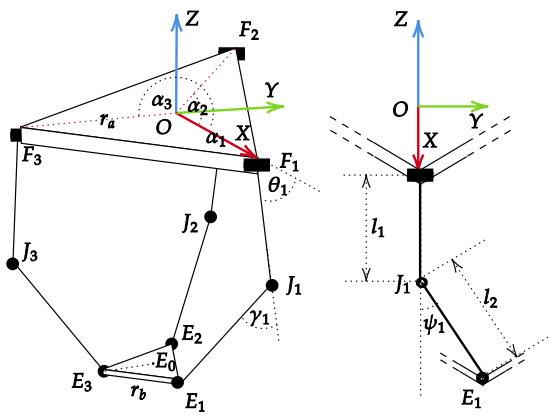

Fig. 1. Delta robot geometrical model. α_i, $i \in \{1,2,3\}$ are the rotation angles around the z-axis of the reference frame.

2.1 Forward and Inverse Kinematics

The forward kinematics provides the Cartesian position of E_0 with respect to the reference frame O. In most of the cases, it must be defined without considering the passive angles, due to the lack of encoders in the passive joints. The forward kinematics is a function $\kappa : \mathbb{R}^3 \to \mathbb{R}^3$ which takes as input the values of θ_i and returns the position $E_0 = \{x_0, y_0, z_0\}$. According to Kuo and Huang (2017), assuming each kinematic chain of identical size, with $l_1 = |F_iJ_i|$, $l_2 = |J_iE_i|$, $r_a = |OF_i|$ and $r_b = |E_0E_i|$, the coordinates of E_0 can be computed as the intersection of three spheres with center in $J_i'(x_{J_i'}, y_{J_i'}, z_{J_i'})$ and radius l_2. J_i' corresponds to the position of J_i in an "equivalent" Delta robot with a fixed base of radius $r = r_a - r_b$ and a moving point-like platform in the E_0. The equations of the three spheres are:

$$(x_0 - x_{J_i'})^2 + (y_0 - y_{J_i'})^2 + (z_0 - z_{J_i'})^2 - l_2^2 = 0, \qquad (1)$$

with $x_{J_i'} = (r + l_1\cos\theta_i)\cos\alpha_i$, $y_{J_i'} = (r + l_1\cos\theta_i)\sin\alpha_i$ and $z_{J_i'} = -l_1\sin\theta_i$, where θ_i is the actuated joint rotation angle and α_i defines the rotation of F_i with respect to O in the XY plane. The intersection of these three spheres yields to a quadratic equation on Cartesian coordinates that has two solutions, one belonging to the real half-space $\mathcal{H}_+ := (x, y, z)$ with $z > 0$ and the other belonging to $\mathcal{H}_- := (x, y, z)$ with $z < 0$. According to the reference frame adopted, the end-effector moves in $\mathcal{H}_-$ so the solution that belongs to $\mathcal{H}_+$ is discarded. Please refer to Kuo and Huang (2017) and Tsai (1999) for more details.

The inverse kinematics $\kappa^{-1} : \mathbb{R}^3 \to \mathbb{R}^3$ computes the values of the generalized coordinates θ_1, θ_2 and θ_3 given the Cartesian coordinates $E_0 = \{x_0, y_0, z_0\}$ of the end-effector, expressed with respect to the robot fixed frame O. According to Kuo (2016), the active joint angles can be obtained by solving the equations (1), $i \in \{1,2,3\}$. They can be rewritten as

$$\ell_i \cos\theta_i + p_i \sin\theta_i = n_i,$$

where

$$\ell_i = 2rl_1 - 2l_1x_0\cos\alpha_i - 2l_1y_0\sin\alpha_i,$$
$$p_i = 2l_1z_0,$$
$$n_i = 2rx_0 - 2ry_0\sin\alpha_i + x_0^2 + y_0^2 + z_0^2 + l_1^2 - l_2^2 + r^2.$$

There are four possible solutions. Please refer to Tsai (1999) for further details on how select the right one.

2.2 Velocity and Acceleration Kinematics

The Cartesian velocity $\dot{x} = (\dot{x}_0\, \dot{y}_0\, \dot{z}_0)^T$ and acceleration $\ddot{x} = (\ddot{x}_0\, \ddot{y}_0\, \ddot{z}_0)^T$ are obtained as functions of $\dot{\theta} = (\dot{\theta}_1\, \dot{\theta}_2\, \dot{\theta}_3)^T$ and $\ddot{\theta} = (\ddot{\theta}_1\, \ddot{\theta}_2\, \ddot{\theta}_3)^T$ by

$$\dot{x} = J\dot{\theta}, \quad \ddot{x} = \dot{J}\dot{\theta} + J\ddot{\theta}, \qquad (2)$$

where J and $\dot{J}$ are the Jacobian matrix of the system and its derivative with respect to time, Olsson (2009). Since the identification is done offline, it is possible to use an array of Kalman smoothers to estimate velocities $\dot{\theta}$ and accelerations $\ddot{\theta}$, Muradore and Fiorini (2011), Anderson and Moore (1979).

3. DELTA ROBOT DYNAMICS

The dynamics of a Delta Robot is obtained by solving the Euler-Lagrange equations of the Lagrangian of the system $L(q, \dot{q}) = T(q, \dot{q}) - V(q)$, taking into account that it has to satisfy a holonomic constraint of rigidity (1), given by the mechanical interconnection between the links at the end-effector. As usual, T is the kinetic energy, V is the potential energy and $q = (x_0\, y_0\, z_0\, \theta_1\theta_2\, \theta_3)^T$, $\dot{q} = (\dot{x}_0\, \dot{y}_0\, \dot{z}_0\, \dot{\theta}_1\, \dot{\theta}_2\, \dot{\theta}_3)^T$ are the generalized coordinates and velocities.

3.1 Kinetic and Potential Energy

T is given by the sum of the contributions of T_j, $j \in \{0,1,2\}$ kinetic energies. The active links F_iJ_i are modeled as homogeneous rods of mass m_1, length l_1, with center of mass (CoM) positioned at $l_1/2$. The passive links J_iE_i are modeled as points of mass m_2 attached to the active links' ends, Kuo and Huang (2017). Therefore, the corresponding inertia terms can be written as

$$\mathcal{I}_1 = \frac{1}{3}m_1l_1^2, \quad \mathcal{I}_2 = m_2l_1^2.$$

The end-effector $E_1E_2E_3$ is modeled as a point of mass m_0 in E_0. The kinetic energy contributions are

$$T_0 = \frac{1}{2}m_0\left\|\dot{x}\right\|^2,$$
$$T_1 = \frac{1}{2}\mathcal{I}_1\sum_{i=1}^{3}\dot{\theta}_i^2 = \frac{1}{6}m_1l_1^2\sum_{i=1}^{3}\dot{\theta}_i^2,$$
$$T_2 = \frac{1}{2}\sum_{i=1}^{3}\left(m_2\left\|\dot{x}\right\|^2 + \mathcal{I}_2\dot{\theta}_i^2\right) = \frac{1}{2}m_2\sum_{i=1}^{3}\left(\left\|\dot{x}\right\|^2 + l_1^2\dot{\theta}_i^2\right),$$

where $\|\cdot\|$ denotes the Euclidean norm.

V is obtained similarly. Since the CoMs of the active links are positioned in their middle points, the V_j $j \in \{0,1,2\}$ terms are given by

$$V_0 = m_0gz_0,$$
$$V_1 = \frac{1}{2}m_1g\,l_1\sum_{i=1}^{3}\sin\theta_i,$$
$$V_2 = m_2g\sum_{i=1}^{3}(z_0 + l_1\sin\theta_i),$$

where g is the acceleration of gravity.

3.2 Constrained Lagrangian Dynamics

Let $f(q) = 0$ be the equations (1); in the Euler-Lagrange equations we have to take into account such constraint

$$\frac{d}{dt}\left(\frac{\partial L}{\partial \dot{q}}\right) - \frac{\partial L}{\partial q} = Q + \lambda \frac{\partial f(q)}{\partial q}, \tag{3}$$

where $\lambda = (\lambda_1\, \lambda_2\, \lambda_3)^T$ are the Lagrange multipliers and Q the generalized forces acting on the system. For an exhaustive theoretical justification please refer to the Lagrange-D'Alambert Principle, in Bullo and Lewis (2004). Computing all the derivatives appearing in the left hand side of equation (3), we have

$$\begin{aligned}
\frac{d}{dt}\left(\frac{\partial L}{\partial \dot{x}_0}\right) &= (m_0 + 3m_2)\ddot{x}_0,\\
\frac{d}{dt}\left(\frac{\partial L}{\partial \dot{y}_0}\right) &= (m_0 + 3m_2)\ddot{y}_0,\\
\frac{d}{dt}\left(\frac{\partial L}{\partial \dot{z}_0}\right) &= (m_0 + 3m_2)\ddot{z}_0,\\
\frac{d}{dt}\left(\frac{\partial L}{\partial \dot{\theta}_i}\right) &= \left(\frac{1}{3}m_1 + m_2\right) l_1^2 \ddot{\theta}_i, \qquad i \in \{1,2,3\}\\
\frac{\partial L}{\partial x_0} &= 0,\\
\frac{\partial L}{\partial y_0} &= 0,\\
\frac{\partial L}{\partial z_0} &= -(m_0 + 3m_2)g,\\
\frac{\partial L}{\partial \theta_i} &= -\left(\frac{1}{2}m_1 + m_2\right) g l_1 \cos\theta_i, \qquad i \in \{1,2,3\}.
\end{aligned}$$

The derivatives with respect to Cartesian variables, together with the right-hand side of equation (3), lead to the following system of equations that we express in matrix form as

$$M\ddot{X} - 2A(q)\Lambda = F, \tag{4}$$

with

$$M = \begin{bmatrix} m_0 + 3m_2 & 0 & 0\\ 0 & m_0 + 3m_2 & 0\\ 0 & 0 & m_0 + 3m_2 \end{bmatrix},\ \ddot{X} = \begin{bmatrix} \ddot{x}_0\\ \ddot{y}_0\\ \ddot{z}_0 + g \end{bmatrix}$$

$$A(q) = \begin{bmatrix} a_{11} & a_{12} & a_{13}\\ a_{21} & a_{22} & a_{23}\\ a_{31} & a_{32} & a_{33} \end{bmatrix},\ \Lambda = \begin{bmatrix} \lambda_1\\ \lambda_2\\ \lambda_3 \end{bmatrix},\ F = \begin{bmatrix} F_{x_0}\\ F_{y_0}\\ F_{z_0} \end{bmatrix},$$

where

$$\begin{aligned}
a_{1i} &= x_0 + r\cos\alpha_i - l_1\cos\theta_i\cos\alpha_i,\\
a_{2i} &= y_0 + r\sin\alpha_i - l_1\cos\theta_i\sin\alpha_i,\\
a_{3i} &= z_0 - l_1\sin\theta_i,
\end{aligned}$$

for $i \in \{1,2,3\}$. The derivatives with respect to the joint variables yield the following system

$$I\ddot{\Theta} + G(q) - 2K(q)\Lambda = T, \tag{5}$$

where

$$I = \begin{bmatrix} m_1/3 + m_2 & 0 & 0\\ 0 & m_1/3 + m_2 & 0\\ 0 & 0 & m_1/3 + m_2 \end{bmatrix} l_1^2,\ \ddot{\Theta} = \begin{bmatrix} \ddot{\theta}_1\\ \ddot{\theta}_2\\ \ddot{\theta}_3 \end{bmatrix}$$

$$G(q) = \begin{bmatrix} v_1\\ v_2\\ v_3 \end{bmatrix},\ K(q) = \begin{bmatrix} k_{11} & 0 & 0\\ 0 & k_{22} & 0\\ 0 & 0 & k_{33} \end{bmatrix},\ T = \begin{bmatrix} \tau_1\\ \tau_2\\ \tau_3 \end{bmatrix}.$$

The terms v_i are given by $(m_1/2 + m_2)g\, l_1 \cos\theta_i$ while the terms k_{ii} are equal to $(x_0\cos\alpha_i + y_0\sin\alpha_i + r)\sin\theta_i - z_0\cos\theta_i$ for $i \in \{1,2,3\}$.

Solving the system (4) with respect to Λ, given the external forces contribution F, and substituting the Λ values into equation (5) allows to determine the torques T. In the case of free motion $F = [0\,0\,0]^T$. This model will be called $\mathcal{M}_{KH}$ since it has been derived by Kuo and Huang (2017).

4. MODEL ENHANCEMENTS

The dynamic model described in Section 3 is an approximation of the real robot. In particular, the passive link, which is modeled as a mass point, yields to a noticeable underestimation of the inertia effect. Moreover, the contribution of joint friction is not taken into account at all. These two issues lead to an under-estimation of the real torque computed by the industrial controller of the real robot. In this Section a method to compensate inertia and potential energies through gray-box dynamical parameter identification, and the linear estimation of viscous and Coulomb friction parameters are proposed. Fig. 2 shows the control loop and the identification block.

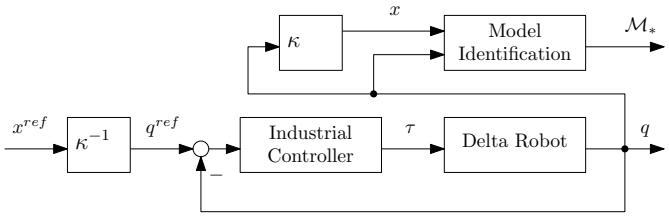

Fig. 2. Control loop with the identification block. $\mathcal{M}_*$ is the identified model

4.1 Gray-box dynamic parameter identification

Two scalar parameters ρ_1 and ρ_2 are added to the dynamic model in order to take into account the missing inertia and potential energy. Equation (5) is accordingly adapted to

$$\rho_1 I\ddot{\Theta} + \rho_2 G(q) - 2K(q)\Lambda = T. \tag{6}$$

In order to fit the best values for ρ_1 and ρ_2, an offline approach has been adopted. The method consists in minimizing the error ε_T between the real robot torques T and the estimated torques $\widehat{T}$, over a set of trajectories Υ. The error minimization is performed with a greedy approach over a range of values between $(\rho_1^{min}, \rho_1^{max})$ and $(\rho_2^{min}, \rho_2^{max})$. In particular, the algorithm cycles through every trajectory $\upsilon \in \Upsilon$, computing the torques T_υ for every $(\rho_1, \rho_2)_\upsilon \in (\rho_1^{min}, \rho_1^{max}) \times (\rho_2^{min}, \rho_2^{max})$, and finds the pair $(\rho_1^\star, \rho_2^\star)_\upsilon$ which minimizes

$$(\rho_1^\star, \rho_2^\star)_\upsilon = \underset{(\rho_1,\rho_2)_\upsilon}{\arg\min}\, \varepsilon_{T_\upsilon} = \mathrm{RMS}(T_\upsilon - \widehat{T}_\upsilon). \tag{7}$$

The overall optimal values $\rho_1^\star$ and $\rho_2^\star$ to be included in (6) are given by the average

$$(\rho_1^\star, \rho_2^\star) = \frac{\sum_\upsilon (\rho_1^\star, \rho_2^\star)_\upsilon}{|\Upsilon|},$$

where $|\Upsilon|$ is the cardinality of Υ.

The enhanced model taking into account the parameters $\rho_1^\star$ and $\rho_2^\star$ will be referred as $\mathcal{M}_{Id}$.

4.2 Friction coefficients identification

Friction plays an important role in determining the torques when the robot operates at high speed, as in the case of Delta robots. Coulomb and viscous friction models, as reported by Khan et al. (2017), account for the fundamental modeling of friction at joints. Equation (6) is modified in order to consider the joint friction contribution as follows:

$$\rho_1 I\ddot{\Theta} + \rho_2 G(q) - 2K(q)\Lambda + B\dot{\Theta} + S\,\mathrm{sign}(\dot{\Theta}) = T, \quad (8)$$

where

$$B = \begin{bmatrix} f_{v1} & 0 & 0 \\ 0 & f_{v2} & 0 \\ 0 & 0 & f_{v3} \end{bmatrix}, \quad S = \begin{bmatrix} f_{c1} & 0 & 0 \\ 0 & f_{c2} & 0 \\ 0 & 0 & f_{c3} \end{bmatrix}.$$

B and S contain the viscous and Coulomb friction coefficients, f_{v_i} and f_{c_i}, respectively. The coefficients are estimated via Least Squares method, Åström and Wittenmark (2013). For every actuated joint a linear regression is performed to estimate the joint friction coefficients. For every $\upsilon \in \Upsilon$, let $|\upsilon|$ be the number of samples in υ. Let $\tau_{\upsilon,i} \in \mathbb{R}^{|\upsilon|\times 1}$ and $\hat{\tau}_{\upsilon,i} \in \mathbb{R}^{|\upsilon|\times 1}$ be the time series of measured torques and computed torques, for joint i, at every sample time, respectively. Let $\dot{\theta}_{\upsilon,i} \in \mathbb{R}^{|\upsilon|\times 1}$ be the vector of i-th joint angular velocity, at every sample time. For the sake of simplicity, from now on, the joint index i will be omitted. Defining

$$\Delta\tau_\upsilon = \tau_\upsilon - \hat{\tau}_\upsilon,$$
$$\Phi_\upsilon = \left[\dot{\theta}_\upsilon \;\; \mathrm{sign}(\dot{\theta}_\upsilon)\right],$$

we have the following linear system

$$\Delta\tau_\upsilon = \Phi_\upsilon \begin{bmatrix} f_c \\ f_v \end{bmatrix}_\upsilon.$$

The viscous and Coulomb friction coefficients are estimated by

$$\begin{bmatrix} f_c^\star \\ f_v^\star \end{bmatrix}_\upsilon = (\Phi_\upsilon^T \Phi_\upsilon)^{-1} \Phi_\upsilon^T \Delta\tau_\upsilon,$$

and, finally,

$$\begin{bmatrix} f_c^\star \\ f_v^\star \end{bmatrix} = \frac{\sum_\upsilon [f_c \;\; f_v]_\upsilon^T}{|\Upsilon|}.$$

are the averages over all the trajectories. The enhanced model taking into account the parameters $\rho_1^\star$ and $\rho_2^\star$ and the friction terms will be referred as $\mathcal{M}_{Id+F}$.

5. PAYLOAD IDENTIFICATION

Delta robots are largely used in the manufacturing industry for high-speed pick-and-place tasks. When an object is picked, the dynamic model needs to be modified accordingly to return the correct values of torques to be provided as feedforward signal to the control architecture. In industrial applications, robots may need to pick objects of unknown sizes and weights resulting in a loss of precision in the torque computation. The purpose of this section is to present a real-time method to identify the payload to increase the accuracy during these specific tasks. Equation (4) (with $F = 0$) should be modified to explicitly consider the payload m_p as

$$M\ddot{X} + M_p\ddot{X} - 2A(q)\Lambda = 0, \quad (9)$$

where

$$M_p = \begin{bmatrix} m_p & 0 & 0 \\ 0 & m_p & 0 \\ 0 & 0 & m_p \end{bmatrix}.$$

Substituting $\Lambda = \frac{1}{2}A(q)^{-1}(M + M_p)\ddot{X}$ from (9) in (5), we get

$$I\ddot{\Theta} + G(q) - K(q)A(q)^{-1}(M + M_p)\ddot{X} = T.$$

Denoting the torque error as $\Delta T = T - \widehat{T}$, where

$$\begin{aligned}\widehat{T} &= I\ddot{\Theta} + G(q) - K(q)A(q)^{-1}M\ddot{X} \\ &= I\ddot{\Theta} + G(q) - 2K(q)\Lambda\end{aligned}$$

is the computed torque without payload, we end up with

$$-A(q)K(q)^{-1}\Delta T = M_p\ddot{X}. \quad (10)$$

Defining[1] $y(k) = -A(k)K(k)^{-1}\Delta T(k)$, the Least Square problem to be solved to estimate M_p is given by

$$\min_{\widehat{M}_p} \sum_k \|y(k)^T - \ddot{X}(k)^T\widehat{M}_p\|^2,$$

where $t = kT_s$ is the current time with T_s the sample time of the controller. As shown in Åström and Wittenmark (2013), the recursive method to solve a least-square problem is more computationally efficient when the observations are obtained sequentially, as in the case of a delta robot picking and releasing objects. Therefore, the current estimation $\widehat{M}_p(k)$ is given by the recursive equation

$$\widehat{M}_p(k+1) = \widehat{M}_p(k) - \mathcal{K}(k)\left(y(k)^T - \ddot{X}(k)^T\widehat{M}_p(k)\right), \quad (11)$$

where

$$\mathcal{K}(k) = \mathcal{P}(k)\ddot{X}(k+1)\left(\sigma + \ddot{X}(k+1)^T\mathcal{P}(k)\ddot{X}(k+1)\right)^{-1},$$
$$\mathcal{P}(k) = \frac{1}{\sigma}\left(I - \mathcal{K}(k-1)\ddot{X}(k)^T\right)\mathcal{P}(k-1).$$

The value $\sigma \in [0, 1]$ is the forgetting factor. With a fine-tuned σ, the model can adapt the torques accordingly with the payload very fast.

6. EXPERIMENTAL RESULTS

This section contains a detailed description of the tests to validate the effectiveness of the dynamic models described in previous sections. To estimate the goodness of a model, the torque profile of each model has been compared to the real torque profile of a D3-1200 Delta robot manufactured by SIPRO Srl using an industrial controller, over a set of trajectories. A Net Analyzer, over Ether-CAT, allowed the recording of kinematic information, commanded and executed torques. The recorded torque values are already multiplied by the motor gear ratio. The recorded data act as ground truth to verify the goodness of each model presented in this paper. The models have been tested on two kinds of trajectories:

- υ_F is a free-motion trajectory, without payload. It contains movements intended to stress the robot, *e.g.* large accelerations and movements close to the workspace bounds. This trajectory is used to show the improvements between the models $\mathcal{M}_{KH}$, $\mathcal{M}_{Id}$ and $\mathcal{M}_{Id+F}$.
- υ_P is a free-motion trajectory, with a payload of 3.8kg at the end-effector. The trajectory contains movements from a standard pick-and-place procedure between two industrial conveyors. This trajectory is used to show the behavior of the model $\mathcal{M}_{Id+F}$ in case of trajectory with/without a payload.

[1] To simplify the notation, we set $A(q(k)) = A(k)$ and $K(q(k)) = K(k)$.

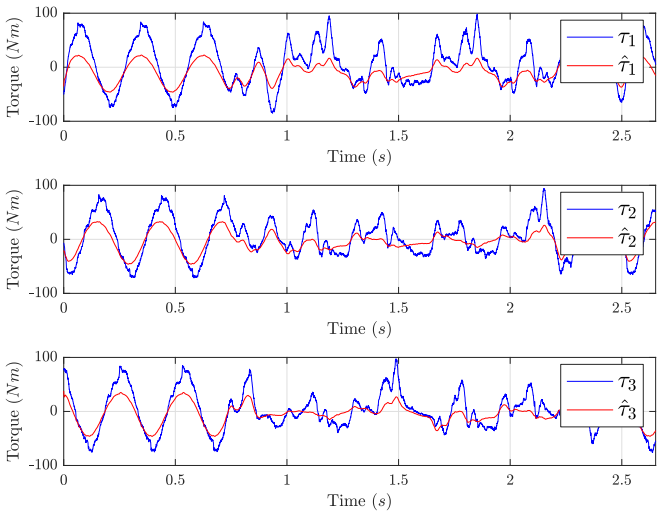

Fig. 3. Torques τ compared with estimated torques $\hat{\tau}$ computed by the model $\mathcal{M}_{KH}$, for each actuated joint over trajectory υ_F.

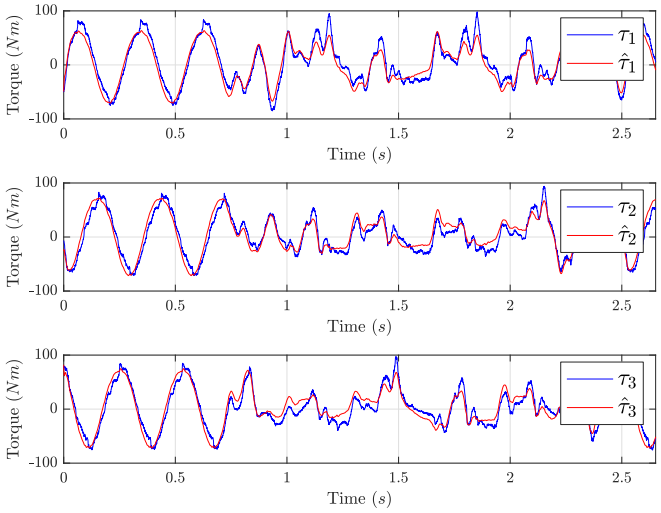

Fig. 4. Torques τ compared with estimated torques $\hat{\tau}$ computed by the model $\mathcal{M}_{Id}$, for each actuated joint over trajectory υ_F.

The model $\mathcal{M}_{KH}$ has been tested on the trajectory υ_F. Fig. 3 shows the torque profiles $\hat{\tau}_i$ and the real robot torques τ_i. The dynamical model underestimates the real torques, due to the model simplifications highlighted in Section 4.

The application of gray-box dynamic parameter identification (Section 4.1), over a set of 12 trajectories, allowed to identify the optimal parameters $\rho_1^\star$ and $\rho_2^\star$. The same trajectory υ_F is used to compare the model with the identified parameters $\mathcal{M}_{Id}$ and $\mathcal{M}_{KH}$. Fig. 4 shows the identified model torque time series $\hat{\tau}_i$ with respect to the torques τ_i. The dynamic parameters $\rho_1^\star$ and $\rho_2^\star$ allow to compensate for the lack of inertia and potential energy in the previous model. The model can follow more accurately the robot torque profile. The total absence of friction modeling is noticeable, especially when the robot is moving at low and high velocities. In those cases, the error between the real and computed torques increases.

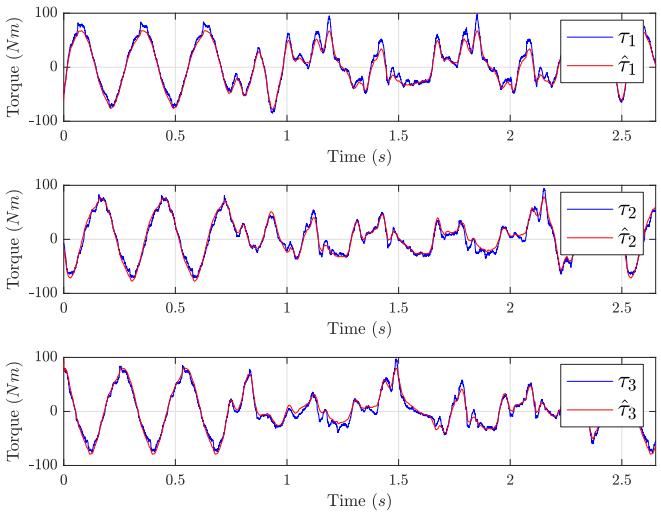

Fig. 5. Torques τ compared with estimated torques $\hat{\tau}$ computed by the model $\mathcal{M}_{Id+F}$, for each actuated joint over trajectory υ_F.

Table 1. Mean error and standard deviation of each model over υ_F

	$\mathcal{M}_{KH}$		$\mathcal{M}_{Id}$		$\mathcal{M}_{Id+F}$	
	μ	σ	μ	σ	μ	σ
τ_1 (Nm)	14.32	23.97	3.62	11.89	3.94	5.67
τ_2 (Nm)	7.98	20.30	-1.09	11.55	-1.11	5.79
τ_3 (Nm)	6.62	20.23	-2.10	11.91	-1.49	6.06

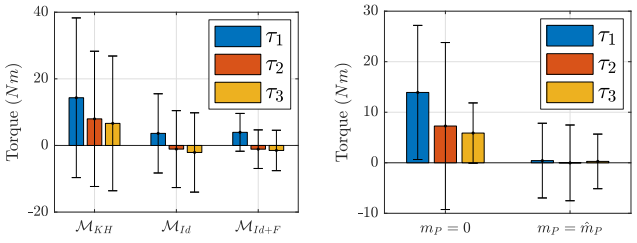

Fig. 6. Mean errors with standard deviations. In (a) each label represents the errors between the dynamical model $\mathcal{M}_*$ and the real robot torque profile. In (b) each label represents the errors between the dynamical model $\mathcal{M}_{Id+F}$ and the real robot torque profile with $m_P = 0$ and $m_P = \hat{m}_P$.

The implementation of the friction estimation method of Section 4.2 brings to the third model $\mathcal{M}_{Id+F}$. The matrices B and S allow to increase the overall model accuracy. The dynamic model with the previously identified dynamic parameters and the new friction coefficients $\mathcal{M}_{Id+F}$ is compared to $\mathcal{M}_{KH}$ over trajectory υ_F. Fig. 5 shows the dynamical model enriched with friction computation $\hat{\tau}_i$, with respect to the real robot torque τ_i. The estimated torques by the mathematical model $\mathcal{M}_{Id+F}$ follow the real torques much better, both at high and low velocities. The mean μ and the variance σ of the error $e(k) = \tau(k) - \hat{\tau}(k)$ have been drastically reduced as shown in Table 1. Fig. 6(a) displays the values in the table.

Until now, each model has been tested in free-motion with no payload. In case of pick-and-place tasks with heavy payloads, the performance would decrease, since the model

Table 2. Mean error and standard deviation of the $\mathcal{M}_{Id+f}$ torque and real τ, over the trajectory υ_P, with $m_P = 0$ and $m_P = \hat{m}_P$.

	$m_P = 0$		$m_P = \hat{m}_P$	
	μ	σ	μ	σ
τ_1 (Nm)	13.91	13.27	0.42	7.39
τ_2 (Nm)	7.27	16.52	-0.02	7.49
τ_3 (Nm)	5.88	5.96	0.27	5.40

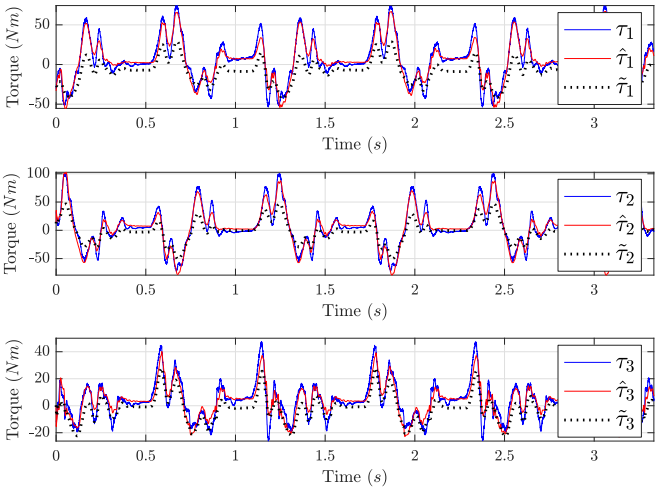

Fig. 7. Torques τ compared with estimated torques $\hat{\tau}$ and $\tilde{\tau}$ computed by the model $\mathcal{M}_{Id+F}$ with and without payload identification, over the trajectory υ_P.

does not take into consideration the different weights at the end-effector.

The purpose of the Payload identification method is to increase the accuracy when the lifted payload m_P is greater than zero. Fig. 7 shows the torques of the dynamic model $\mathcal{M}_{Id+F}$ with the identified payload information $\hat{\tau}_i$, at run-time, compared to the dynamical model without this information, $\tilde{\tau}_i$, and the real robot torques τ_i. The test has been executed over the trajectory υ_P. Fig. 8 shows the estimated payload $\hat{m}_p$ using the method (11). This model achieves good results in terms of transient time and accuracy. Table 2 shows the values of the mean error and standard deviation of the torque error with $m_P = \hat{m}_P$ and without payload, $m_P = 0$. Fig. 6(b) displays the values in the table and shows the reduction of the errors when the payload m_P is correctly computed.

7. CONCLUSIONS

Starting from an approximated model and using gray-box dynamic parameter identification and friction modelling, we obtained a better mathematical model of Delta robots. Since Delta robot are mostly used in pick-and-place tasks, it has been proposed a method which adjusts the dynamic parameters in order to estimate the payload contribution in terms of computed torques, i.e. the mass of the payload at the end-effector. Future research will focus on the implementation of a feedforward torque control loop, based on the identified dynamical model (Fig. 9).

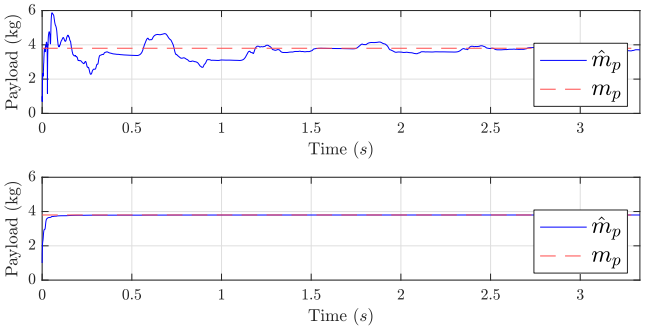

Fig. 8. Payload estimation over time. The mass $\hat{m}_p$ is the estimated payload, while m_p is the correct payload attached to the end-effector. The top graph shows the estimation using the real torque measurements whereas the bottom graph shows the estimation using the simulated torque of the $\mathcal{M}_{Id+F}$ model.

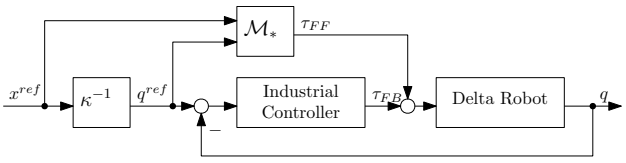

Fig. 9. Control loop with feed-forward torque τ_{FF} based on the identified model $\mathcal{M}_*$ and feedback torque τ_{FB}.

REFERENCES

Anderson, B.D. and Moore, J.B. (1979). Optimal filtering. *Prentice-Hall*.

Åström, K.J. and Wittenmark, B. (2013). *Computer-controlled systems: theory and design*. Courier Corporation.

Bortoff, S.A. (2018). Object-oriented modeling and control of delta robots. In *2018 IEEE Conference on Control Technology and Applications (CCTA)*, 251–258. IEEE.

Bullo, F. and Lewis, A.D. (2004). *Geometric control of mechanical systems: modeling, analysis, and design for simple mechanical control systems*, volume 49. Springer Science & Business Media.

Khan, Z.A., Chacko, V., and Nazir, H. (2017). A review of friction models in interacting joints for durability design. *Friction*, 5(1), 1–22.

Kuo, Y.L. (2016). Mathematical modeling and analysis of the delta robot with flexible links. *Computers & Mathematics with Applications*, 71(10), 1973–1989.

Kuo, Y.L. and Huang, P.Y. (2017). Experimental and simulation studies of motion control of a delta robot using a model-based approach. *International Journal of Advanced Robotic Systems*, 14(6), 1–14.

Muradore, R. and Fiorini, P. (2011). A PLS-based statistical approach for fault detection and isolation of robotic manipulators. *IEEE Transactions on Industrial Electronics*, 59(8), 3167–3175.

Olsson, A. (2009). Modeling and control of a delta-3 robot. *MSc Theses*.

Staicu, S. and Carp-Ciocardia, D.C. (2003). Dynamic analysis of Clavel's Delta parallel robot. In *2003 IEEE International Conference on Robotics and Automation*, volume 3, 4116–4121.

Tsai, L.W. (1999). *Robot analysis: the mechanics of serial and parallel manipulators*. John Wiley & Sons.